Broad cytotoxic targeting of acute myeloid leukemia by highly polyclonal Delta One T cells

Biagio Di Lorenzo[1,2]*, André E. Simões[1,3]*, Francisco Caiado[1], Paola Tieppo[4], Daniel V. Correia[1,5], Tânia Carvalho[1], Maria Gomes da Silva[6], Julie Déchanet-Merville[7], Ton Schumacher[8], Immo Prinz[9], Haakan Norell[1], Sarina Ravens[9], David Vermijlen[4] and Bruno Silva-Santos[1]

[1]Instituto de Medicina Molecular João Lobo Antunes, Faculdade de Medicina, Universidade de Lisboa, Lisbon, Portugal

[2]Instituto Superior Técnico, Universidade de Lisboa, Lisbon, Portugal

[3]Lymphact – Lymphocyte Activation Technologies S.A., Coimbra, Portugal

[4]Department of Pharmacotherapy and Pharmaceutics, Institute for Medical Immunology, Université Libre de Bruxelles, Brussels, Belgium

[5]GammaDelta Therapeutics, London, United Kingdom

[6]Instituto Português de Oncologia – Francisco Gentil, Lisbon, Portugal

[7]Immunoconcept, CNRS UMR 5164 , Université de Bordeaux, Bordeaux, France

[8]Netherlands Cancer Institute, Amsterdam, The Netherlands

[9]Hannover Medical School, Hannover, Germany

Keywords: Acute Myeloid Leukemia, Immunotherapy, Adoptive Cell Transfer, Gamma-Delta T cells

Correspondence:

Prof. Bruno Silva-Santos
Instituto de Medicina Molecular João Lobo Antunes
Faculdade de Medicina, Universidade de Lisboa
Avenida Prof. Egas Moniz
1649-028 Lisboa, Portugal
E-mail: bssantos@medicina.ulisboa.pt

Abstract

Acute myeloid leukemia (AML) remains a major clinical challenge due to frequent chemotherapy resistance and deadly relapses. We are exploring the immunotherapeutic potential of peripheral blood Vδ1$^+$ T-cells, which associate with improved long-term survival of stem-cell transplant recipients, but have never been applied as adoptive cell therapy. Using our recently developed clinical-grade protocol for expansion and differentiation of “Delta One T” (DOT) cells, we found them to be highly cytotoxic against AML primary samples and cell lines, including cells selected for resistance to standard chemotherapy. Interestingly, unlike chemotherapy, DOT-cell targeting did not select for outgrowth of specific AML lineages, suggesting a broad recognition domain, which was also consistent with the striking polyclonality of the DOT-cell TCR repertoire. Moreover, whereas AML reactivity was only slightly impaired upon anti-Vδ1$^+$ TCR antibody blockade, it was strongly dependent on expression of the NKp30 ligand, B7-H6. In contrast, DOT-cells did not show any reactivity against normal leukocytes, including CD33$^+$ or CD123$^+$ myeloid cells. Importantly, adoptive transfer of DOT-cells *in vivo* markedly reduced AML load in the blood and target organs of multiple human AML xenograft models; and significantly prolonged host survival, without any noticeable toxicity, thus providing the proof-of-concept for DOT-cell application in AML treatment.

INTRODUCTION

Acute myeloid leukemia (AML) has a dismal (10%) survival rate among the elderly, mostly due to resistance to standard treatment. This consists in a combination of cytarabine with an anthracyclin drug, which while effective at inducing complete remissions, ultimately selects chemoresistant clones that drive refractory relapses(1,2). Promising alternatives to chemotherapy are novel targeted therapies(1,3) and upcoming immunotherapies(2), especially chimeric antigen receptor (CAR) T-cell transfer, fueled by notable recent success in B-cell malignancies(4). However, CARs have proved difficult to implement in AML mainly due on-target effects on vital healthy myeloid progenitor cells that express the target antigens CD33 and CD123(2). By contrast, we are focusing on *ex vivo* differentiated Delta One T (DOT) cells that rely on physiological receptors, namely T cell receptor (TCR) and natural cytotoxicity receptors (NCR) such as NKp30 and NKp44, to distinguish transformed from healthy cells(5–7). Importantly, DOT-cells are derived from peripheral blood $V\delta1^+$ $\gamma\delta$ T-cells, whose *in vivo* expansion correlated with enhanced long-term disease-free survival of leukemia patients that received allogeneic hematopoietic stem cell transplantation(8).

While the clinical manipulation of $V\delta1^+$ $\gamma\delta$ T-cells has been hindered by their relatively low abundance (<0.5%) among peripheral blood lymphocytes, we recently devised the first clinical-grade protocol to expand and differentiate large numbers of DOT-cells endowed with potent anti-tumor cytotoxicity(5,6). Thus, our 3-week protocol achieves > 1,000-fold expansions of $V\delta1^+$ $\gamma\delta$ T-cells, for which the synergistic action of TCR and IL-4 stimulation is critical (during its 1^{st} stage), whereas the 2^{nd} stage focuses on the IL-15-dependent differentiation of potent anti-tumor DOT-cell effectors endowed with NCR expression(6). Converging the properties and potential of DOT-cells with the unmet immunotherapy needs of AML, in this study we aimed to purpose DOT-cells specifically for AML treatment.

MATERIALS AND METHODS

Ethics statement

Primary AML cells were obtained from the peripheral blood of patients at first presentation, after informed consent and institutional review board approval. The study was conducted in accordance with the Declaration of Helsinki.

Mice

NOD SCID $\gamma_c^{-/-}$ (NSG), NOD SCID $\gamma_c^{-/-}$ SGM3 (NSGS), and NOD Rag1$^{-/-}$ $\gamma_c^{-/-}$ SGM3 (NRGS) mice were obtained from the Jackson Laboratories. Age and sex-matched mice were randomly distributed among the different groups. Disease development was followed through weekly bleedings (in intra-bone marrow models) and disease end-point is achieved upon first indication of back leg decreased mobility. All animal procedures were performed in accordance to national guidelines from the Direção Geral de Veterinária and approved by the Animal Ethics Committee of Instituto de Medicina Molecular João Lobo Antunes.

DOT-cell production and TCR repertoire analysis

DOT-cells were produced from peripheral blood of healthy donors, cultured for 21 days as previously detailed(6). In brief, MACS-sorted γδ T cells were resuspended in serum-free culture medium (OpTmizer-CTS) supplemented with 5% autologous plasma and 2mM L-glutamine (Thermo Fischer Scientific). Animal-free human cytokines (100ng/ml rIL-4, 70ng/ml rIFN-γ, 7ng/ml rIL-21 and 15ng/ml rIL-1β; all from Peprotech) and a soluble antibody (70ng/ml anti-CD3 mAb, clone OKT-3; BioXcell) were added to the medium. Cells were incubated at 37ºC and 5% CO_2. Every 5-6 days, old medium was removed and replaced with fresh medium supplemented with cytokines (including 70ng/ml rIL-15 and 30ng/ml IFN-γ), and with 1µg/ml anti-CD3 mAb.

For *TRGV* and *TRDV* repertoire analysis, V$\delta1^+$ T cells were FACS-sorted either from the initial blood sample (*ex vivo*); or from the final (3-week culture)

DOT-cell product. Next-generation sequencing was performed as previously described(9,10). The software for data analysis is described in Supplementary Table 4.

For DOT-cell clone generation, $CD3^+$ $TCRV\delta1^+$ $TCRV\delta2^-$ single cells were FACS-sorted into 96 wells/plates; and cultured for 21 days using the DOT-cell protocol in the presence of (weekly-renewed) 10^4 irradiated autologous PBMCs (feeders).

AML cell targeting in vitro and in vivo

AML cell lines (Supplementary Table 3) were obtained from and authenticated by the German Resource Center for Biologic Material (DSMZ). Lentiviral barcoding of AML cells was performed and analyzed as previously detailed(11). For *in vitro* targeting, AML cell lines or primary samples were co-incubated with DOT-cells for 3 hours; and stained with Annexin-V, as detailed(6). For *in vivo* targeting, three xenograft hAML models were established as represented in Supplementary Figure 9. The patient-derived xenograft (intra-tibia injection) was recently described(12). Tumor burden was assessed by staining with anti-human CD45 (HI30) and CD33 (P67.6) antibodies. Flow cytometry acquisition was performed on a LSR Fortessa (BD) and data was analyzed with FlowJo X software (Tree Star).

CRISPR/ Cas9 knockout

Guide RNAs (gRNA1: CACCGTTCCGGACCACCGTTATAAC; gRNA2: CACCGGGGCTCTGATCCAATATGAT) were designed to target the genomic sequence of B7-H6 in two areas close to the promoter. gRNAs were inserted into a plasmid containing the sequence codifying for Cas9 enzyme and transfected by electroporation in HEL cells. Successful single cell knockout clones were confirmed by qRT-PCR (forward primer: CACAGGGAACAGTCCAGCTT; reverse primer TGATCCAGCAACAATCTGCT, performed as previously described (5).

Statistical analysis

Performed using GraphPad Prism software. All data expressed as mean +/- SEM. Comparisons of two groups by Student's t-test; and more than two groups by ANOVA test with Dunnet's post test. Animal survival comparisons performed using Log-rank (Mantel-Cox) test.

Data sharing

The data have been deposited with links to BioProject accession number PRJNA491919 in the NCBI BioProject database (https://www.ncbi.nlm.nih.gov/bioproject/); the sample list is available as Supplementary Table 5.

RESULTS AND DISCUSSION

On our path to developing a novel Vδ1$^+$ γδ T-cell-based adoptive cell therapy for cancer(5,6), we started this study by further characterizing the DOT-cell product upon expanding αβ-depleted PBMCs with the established DOT-cell protocol (6) and analyzing Vδ1$^+$ T-cell percentages and numbers along with NCR expression over time (Supplementary Figure 1 and Supplementary Table 1). Since recent reports described the clonal expansion and focusing of the adult peripheral blood Vδ1$^+$ T-cell repertoire(13), likely driven by common pathogens such as CMV(10), we questioned the impact of the DOT-cell expansion/ differentiation process on TCR repertoire by performing next generation sequencing of the CDR3 regions in *TRGV* and *TRDV* genes, before and after the 3-week cultures. Strikingly, we found DOT-cells to be extremely polyclonal and thus devoid of dominant clones, in stark contrast to *ex vivo* Vδ1$^+$ T-cells from all donors analyzed (Figure 1A-B and Supplementary Figure 2). This was clearly illustrated by the contribution of the top 20 expanded clones to the overall Vδ1$^+$ TCR repertoire: whereas they represented >60% in the peripheral blood, they accounted for less than 10% in the DOT-cell products (Figure 1C). Moreover, the contribution of individual *TRGV* and *TRDV* chains to the *ex vivo* and DOT-cell repertoires was different (Supplementary Figure 3); and very few clonotypes (especially for *TRDV*) were shared between those identified *ex vivo* and in DOT-cells (Supplementary Table 2). We next aimed to better understand the basis for the remarkable diversification of the DOT-cell repertoire. Given the previous association of CD27 downregulation with pre-expanded/ differentiated Vδ1$^+$ T-cells(13), we compared the TCR clonality of DOT-cells produced from pre-sorted CD27(-) versus CD27(+) subsets, which consistently displayed distinct proliferation capacities under the DOT-cell protocol (Figure 1D). We found that the generation of highly diverse DOT-cells was restricted to CD27(+) precursors (Figure 1E-F; Supplementary Figure 4). Taking into account that CD27(+) cells typically represent only a small fraction of *ex vivo* Vδ1$^+$ T-cells (Supplementary Figure 5A), these data suggest that the DOT-cell protocol preferentially expands naïve-like CD27(+) Vδ1$^+$ T-cells with an extremely diverse TCR repertoire, at the expense of pre-expanded and terminally

differentiated CD27(-) Vδ1$^+$ T-cells. In support of this, the DOT-cell population (generated from bulk Vδ1$^+$ T-cells) was almost entirely composed of CD27(+) cells (Figure 1G). Of note, DOT-cell products originated from pre-sorted CD27(+) cells expressed NKp30 and were highly cytotoxic against KG-1 AML cells (Supplementary Figure 5B-C).

To assess the functional relevance of DOT-cell polyclonality, we generated clones from single-cell sorted Vδ1$^+$ T-cells, expanded/ differentiated using an adapted DOT-cell protocol including the addition of feeder cells to support expansion from single-cells (Supplementary Figure 6); and tested their cytotoxicity against the AML cell line KG-1 (Figure 2A). Strikingly, we found the vast majority of clones (from different donors) to be highly efficient at inducing apoptosis of KG-1 cells upon short (3-hour) co-incubation *in vitro* (Figure 2A). These results show that DOT-cell products are composed of multiple clones with intrinsic capacity to target AML cells. To functionally test if the TCR is involved in this reactivity, we performed the killing assay in the presence of an anti-Vδ1$^+$ TCR specific blocking monoclonal antibody (or isotype control), and observed only a mild reduction in KG-1 cell targeting across a number of clones from different donors (Figure 2B). At this stage we hypothesized that most of the reactivity was mediated by natural cytotoxicity receptors(5–7), particularly NKp30 (Supplementary Figure 1F). In fact, DOT-cell cytotoxicity was significantly decreased upon CRISPR/ Cas9-mediated knockout of the best established tumor-associated NKp30 ligand, B7-H6, in target AML cells (Figure 2C-D).

In order to further evaluate the anti-AML activity, we tested bulk DOT-cell products (from multiple donors) against various other AML cell lines (Supplementary Table 3) as well as primary samples obtained from patients at diagnosis. In all cases, DOT-cells readily (within 3 hours) killed AML cells *in vitro* (Figure 3A-B), in similar fashion to what was reported for CAR-T cells(14–16), and clearly unlike *ex vivo* Vδ1$^+$ T cells (Supplementary Figure 7). Of note, DOT-cell cytotoxicity clearly associated with increased degranulation and expression of perforin and granzyme B upon tumor cell recognition (Supplementary Figure 8). Critically, DOT-cells did not target any normal leukocyte population (neither myeloid nor lymphoid) from the

peripheral blood of healthy volunteers (Figure 3C), including $CD33^+$ and $CD123^+$ myeloid progenitor cells whose on-target depletion by the respective CAR-T cells is known to be responsible for the unwanted myeloablation(2,15).

To test DOT-cells against AML *in vivo*, we established various independent xenograft models of AML (Supplementary Figure 9). Strikingly, both in AML cell line models (Figure 3D-E; Supplementary Figure 9C) and in two patient-derived xenografts (Figure 3F-G; Supplementary Figure 9D-E), DOT-cell treatment markedly reduced tumor burden and increased host survival, without any noticeable toxicity. While CAR-T cells have been reported to produce bigger survival benefits in AML xenografts (14–16), these models were biased to AML cell lines uniformly expressing the target antigens. Furthermore, and critically, xenografts cannot evaluate the toxicity of a strategy predicted to induce myeloablation in patients. Overall, we believe that the combined safety and efficacy profiles of DOT-cells make them very attractive candidates for adoptive cell therapy of AML in the near future.

On the other hand, at the present time, the major therapeutic problem in AML is chemoresistance, which drives deadly relapses. We next asked whether DOT-cells could target chemoresistant AML cells. For that purpose, we subjected AML cells to high doses of cytarabine plus doxorubicin for 72h, which led to >99% tumor cell elimination; and then allowed the survivors to re-grow before re-treating them with chemotherapy or DOT-cells. Whereas the cytotoxic efficacy of chemotherapy was drastically reduced, that of DOT-cells was not impacted (Figure 4A), demonstrating the superior capacity of DOT-cells to target chemoresistant AML cells. In light of this, and taking into account the highly polyclonal and multireactive DOT-cell repertoire (Figure 1A-C), we also questioned the ability of DOT-cells to re-target AML cells following a first DOT-cell treatment that eliminated >99% tumor cells in 72h (Figure 4B). Thus, we FACS-sorted the remaining ~0.1% of AML cells present at 72h and allowed them to re-grow before re-treatment with DOT-cells. Interestingly, DOT-cells killed DOT-pre-treated AML cells as efficiently as non-treated controls (Figure 4C), suggesting that DOT-cell treatment did not select for a specific subset of DOT-resistant AML cells. To track the AML clonal dynamics upon therapeutic (DOT-cells or chemotherapy) pressure, we tagged

single AML cells with cellular barcodes (non-coding DNA sequences that can be tracked by NGS)(11). Interestingly, whereas chemotherapy selectively targeted approximately half of all barcoded AML single-cell lineages, DOT-cells mostly preserved the clonal architecture of the AML population (Figure 4D-E). These data collectively suggest that the breadth of AML targeting based on many cytotoxic DOT-cell clones avoids the selection of resistant lineages and allows efficient re-treatment. Given the urgency of preventing the emergence of deadly refractory relapses, namely after standard chemotherapy, our work provide strong pre-clinical proof-of-concept for clinical application of DOT-cells in AML treatment.

Acknowledgements

We thank Inês Barbosa (IPO Lisboa) for help with provision of primary AML samples; Simão Rocha and Teresa F. Mendes for technical help; Diogo R. Anjos and Natacha G. Sousa for administrative support; and the Animal and Flow Cytometry facilities of iMM-JLA for technical assistance. Our work was funded by Fundação para a Ciência e Tecnologia (PTDC/DTP-PIC/4931/2014 to B.S.S; PD/BD/105880/2014 to B.D.L; BPD/85947/2012 to D.V.C.); Lymphact S.A. (upon investment from Portugal Capital Ventures, S.A, and Busy Angels SCR); GammaDelta Therapeutics (Sponsored Research Agreement to B.S.-S.); and Télévie-FNRS (7.4555.14F to D.V.). We also acknowledge LISBOA-01-0145-FEDER-007391 and LISBOA-01-0145-FEDER-016394, projects cofunded by FEDER, through POR Lisboa 2020 - Programa Operacional Regional de Lisboa, PORTUGAL 2020, and Fundação para a Ciência e a Tecnologia.

Authorship contributions

B.S.-S., B.D.L., A.E.S., D.V., S.R. and H.N. designed research; I.P., T.S., J.D.-M. and M.G.S. provided key methodology; B.D.L., A.E.S., F.C., P.T., D.V.C. and T.C. performed research; B.S.-S., B.D.L. and A.E.S. wrote the manuscript.

Disclosure of conflicts of interest

D.V.C. and B.S.-S. are shareholders of GammaDelta Therapeutics.

REFERENCES

1. Wei AH, Tiong IS. Midostaurin, enasidenib, CPX-351, gemtuzumab ozogamicin, and venetoclax bring new hope to AML. Blood. 2017;130:2469–74.
2. Tasian S. Acute myeloid leukemia chimeric antigen receptor T-cell immunotherapy: how far up the road have we traveled? Ther Adv Hematol. 2018;9:135–48.
3. Di Tullio A, Rouault-Pierre K, Abarrategi A, Mian S, Grey W, Gribben J, et al. The combination of CHK1 inhibitor with G-CSF overrides cytarabine resistance in human acute myeloid leukemia. Nat Commun. 2017;8:1679.
4. June C, O'Connor R, Kawalekar O, Ghassemi S, Milone M. CAR T cell immunotherapy for human cancer. Science (80-). 2018;359:1361–5.
5. Correia D, Fogli M, Hudspeth K, Gomes Da Silva M, Mavilio D, Silva-Santos B. Differentiation of human peripheral blood Vδ1+ T cells expressing the natural cytotoxicity receptor NKp30 for recognition of lymphoid leukemia cells. Blood. 2011;118:992–1001.
6. Almeida AR, Correia D V., Fernandes-Platzgummer A, Silva CL da, Silva MG da, Anjos DR, et al. Delta One T cells for immunotherapy of chronic lymphocytic leukemia: clinical-grade expansion/differentiation and preclinical proof-of-concept. Clin Cancer Res. 2016;22:5795–804.
7. Simões A, Di Lorenzo B, Silva-Santos B. Molecular determinants of target cell recognition by human γδ T cells. Front Immunol. 2018;9:929.
8. Godder K, Henslee-Downey P, Mehta J, Park B, Chiang K, Abhyankar S, et al. Long term disease-free survival in acute leukemia patients recovering with increased γδ T cells after partially mismatched related donor bone marrow transplantation. Bone Marrow Transplant. 2007;39:751–7.
9. Verstichel G, Vermijlen D, Martens L, Goetgeluk G, Brouwer M, Thiault N, et al. The checkpoint for agonist selection precedes conventional selection in human thymus. Sci Immunol. 2017;2:pii:eaah4232.

10. Ravens S, Schultze-Florey C, Raha S, Sandrock I, Drenker M, Oberdorfer L, et al. Human γδ T cells are quickly reconstituted after stem-cell transplantation and show adaptive clonal expansion in response to viral infection. Nat Immunol. 2017;18:393–401.

11. Naik SH, Perié L, Swart E, Gerlach C, Van Rooij N, De Boer RJ, et al. Diverse and heritable lineage imprinting of early haematopoietic progenitors. Nature. 2013;496:229–32.

12. Nobrega-Pereira S, Caiado F, Carvalho T, Matias I, Graça G, Gonçalves LG, et al. VEGFR2–mediated reprogramming of mitochondrial metabolism regulates the sensitivity of acute myeloid leukemia to chemotherapy. Cancer Res. 2018;78:731–41.

13. Davey MS, Willcox CR, Joyce SP, Ladell K, Kasatskaya SA, Mclaren JE, et al. Clonal selection in the human Vδ1 T cell repertoire indicates γδ TCR-dependent adaptive immune surveillance. Nat Commun. 2017;8:14760.

14. Mardiros A, Dos Santos C, McDonald T, Brown C, Wang X, Budde L, et al. T cells expressing CD123-specific chimeric antigen receptors exhibit specific cytolytic effector functions and antitumor effects against human acute myeloid leukemia. Blood. 2013;122:3138–48.

15. Gill S, Tasian S, Ruella M, Shestova O, Li Y, Porter D, et al. Preclinical targeting of human acute myeloid leukemia and myeloablation using chimeric antigen receptor-modified T cells. Blood. 2014;123:2343–54.

16. Petrov J, Wada M, Pinz K, Yan L, Chen K, Shuai X, et al. Compound CAR T-cells as a double-pronged approach for treating acute myeloid leukemia. Leukemia. 2018;32:13171326.

FIGURE LEGENDS

Figure 1. DOT-cells display striking clonal diversity

(A-B) Graphical representation of *TRGV* (left) and *TRDV* (right) repertoires and CDR3 length (number of nucleotides) distribution of FACS-sorted Vδ1$^+$ T cells from (A) peripheral blood/ PB; or (B) DOT-cell products (see also Supplementary Figure 2). Each square represents a different clonotype (with distinct nucleotide sequence), its area is proportional to the relative abundance in the sample; and the color groups the clonotypes by chains. **(C)** Contribution of the top 20 clones to the overall Vδ1$^+$ TCR repertoire of each sample (HD1-4, healthy donors 1 to 4). **(D)** Fold expansion of pre-sorted CD27- *versus* CD27+ Vδ1$^+$ T cells after 21 days with the DOT-cell protocol (HD5-6, healthy donors 5 and 6). **(E)** Graphical representation of *TRGV* repertoire and CDR3 length distribution (alike A-B) for CD27- *versus* CD27+ Vδ1$^+$ T cells cultured for 21 days with the DOT-cell protocol (see also Supplementary Figure 4). **(F)** Shannon indices for intra-sample variability of *TRGV* and *TRDV* repertoires from (A-B) and (E). **(G)** Percentage of CD27(+) cells upon expansion with the DOT-cell protocol. Data in this Figure are derived from 6 independent healthy donors.

Figure 2. Clonal DOT-cell reactivity against AML cells

(A-B) *In vitro* killing of AML KG-1 cells by DOT-cell clones generated from single Vδ1$^+$ T cells sorted from healthy donors (see also Supplementary Figure 6). Cells were co-incubated for 3 hours at 10:1 (E:T) ratio and then analyzed by Annexin V staining (percentage of positive events among pre-labeled KG-1 cells). Each bar represents killing of KG-1 cells upon co-incubation with individual clones. Dashed red line represents the mean basal tumor cell death (without DOT-cells). In **(B)**, either anti-Vδ1$^+$ TCR specific monoclonal antibody or isotype control was added to the cultures. Shown are the clones where the blockade led to clearer reduction in KG-1 targeting. Data represent the average of two technical replicates and are derived from 4 independent healthy donors (HD). **(C)** Real-time PCR for B7-H6 mRNA levels

in parental (B7-H6$^{+/+}$) and CRISPR/ Cas9-manipulated (B7-H6$^{-/-}$) AML HEL cell lines. **(D)** *In vitro* killing of B7-H6$^{+/+}$ or B7-H6$^{-/-}$, AML HEL cells by bulk DOT-cells produced from 3 healthy donors (tested in technical duplicates). Cells were co-incubated for 3 hours at 10:1 (E:T) ratio and then analyzed by Annexin-V staining (shown are percentages of positive events among pre-labeled HEL cells). Indicated are mean + SEM, *** $p < 0.001$.

Figure 3. DOT-cells target multiple AML cell types but not healthy leukocytes

(A-C) *In vitro* killing assays with DOT-cells produced from 3-4 healthy donors, co-incubated for 3 hours at 10:1 (E:T) ratio with the indicated AML cell lines (A), primary AML samples (B) or normal leukocyte populations FACS-sorted from the peripheral blood (C). In (A) the dashed red line represents the mean basal tumor cell death; and in (B), CTR refers also to tumor cells alone (without DOT-cells). Experiments were performed with technical triplicates. **(D-G)** *In vivo* AML targeting by DOT-cells. DOT-cells (3 injections of 2 x 10^7 cells, see Supplementary Figure 9) were transferred to NSG mice (n = 6 CTR, 7 DOT treated mice) pre-injected with KG-1 AML cells (D-E); or NSGS mice (n = 5 CTR, 5 DOT treated mice) bearing primary AML cells (F-G; patient-derived xenograft, PDX). Tumor burden was assessed in the blood and liver one week after the last DOT-cell transfer (D); or through weekly bleedings (F). Indicated are mean + SEM, * $p < 0.05$, *** $p < 0.001$, **** $p < 0.0001$. Animals were sacrificed when advanced disease symptoms (such as back leg paralysis) were observed. Survival curves are presented in panels E ($p < 0.05$) and G ($p < 0.01$).

Figure 4. DOT-cells efficiently (re-)target chemotherapy-resistant AML

Comparison of the *in vitro* anti-AML activity of DOT-cells and standard chemotherapy. **(A)** DOT-cells and standard AML chemotherapy (Doxorubicin plus Cytarabine) protocols were tested against chemotherapy-naïve (wild type, wt) or chemo-relapsed (CR, re-grown after >99% HEL cell elimination) AML cells. Shown are the percentages of Annexin V$^+$ HEL cells after 3 hours of treatment. **(B)** Number of AML HEL cells before and after 72 hours of

treatment with DOT-cells (at 5:1 E:T ratio). Surviving cells (<1%) were re-sorted and allowed to re-grow, thus generating the DOT-treated (DT) samples of (C-E). **(C)** DOT-cells were co-incubated for 3 hours with non-treated (NT) or previously DOT-treated (DT) AML HEL cells at 5:1 or 10:1 (E:T) ratios. Shown are the percentages of Annexin V^+ HEL cells. **(D)** Number of barcoded AML single-cell lineages in non-treated (NT), chemotherapy-treated (CT) or DOT-treated (DT) AML HEL cells. **(E)** Pearson correlation for distribution of barcoded AML single-cell lineages between different treatments. Red, yellow and green dashed lines represent low, medium and high correlations, respectively. Indicated are mean + SEM; ** $p < 0.01$, *** $p < 0.001$, **** $p < 0.0001$.

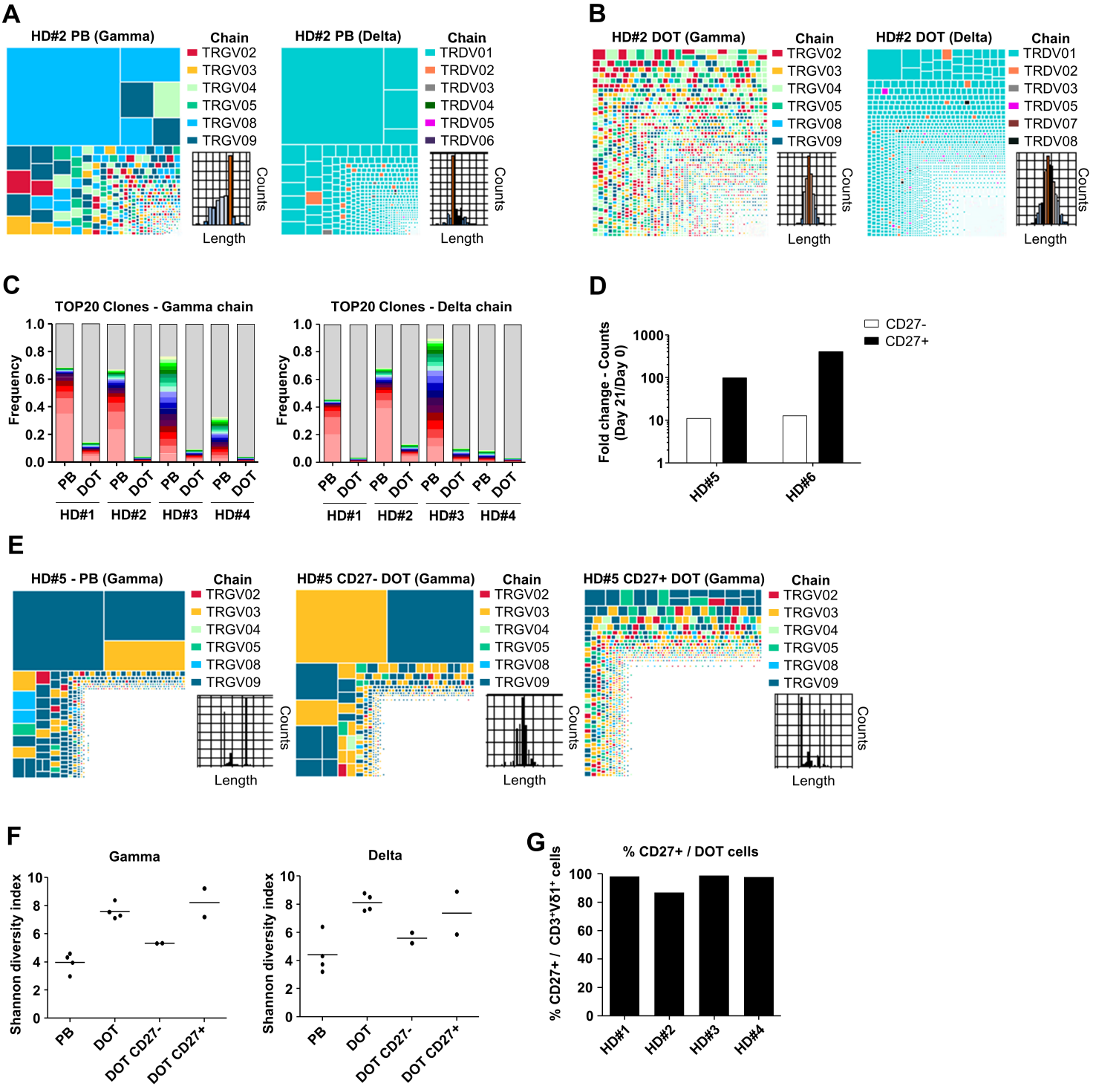
A
HD#2 PB (Gamma)
Chain
TRGV02
TRGV03
TRGV04
TRGV05
TRGV08
TRGV09
Counts
Length
HD#2 PB (Delta)
Chain
TRDV01
TRDV02
TRDV03
TRDV04
TRDV05
TRDV06
Counts
Length
B
HD#2 DOT (Gamma)
Chain
TRGV02
TRGV03
TRGV04
TRGV05
TRGV08
TRGV09
Counts
Length
HD#2 DOT (Delta)
Chain
TRDV01
TRDV02
TRDV03
TRDV05
TRDV07
TRDV08
Counts
Length
C
TOP20 Clones - Gamma chain
Frequency
1.0
0.8
0.6
0.4
0.2
0.0
PB
DOT
HD#1
HD#2
HD#3
HD#4
TOP20 Clones - Delta chain
Frequency
HD#1
HD#2
HD#3
HD#4
D
Fold change - Counts (Day 21/Day 0)
1000
100
10
1
CD27-
CD27+
HD#5
HD#6
E
HD#5 - PB (Gamma)
Chain
TRGV02
TRGV03
TRGV04
TRGV05
TRGV08
TRGV09
Counts
Length
HD#5 CD27- DOT (Gamma)
Chain
TRGV02
TRGV03
TRGV04
TRGV05
TRGV08
TRGV09
Counts
Length
HD#5 CD27+ DOT (Gamma)
Chain
TRGV02
TRGV03
TRGV04
TRGV05
TRGV08
TRGV09
Counts
Length
F
Gamma
Shannon diversity index
10
8
6
4
2
0
PB
DOT
DOT CD27-
DOT CD27+
Delta
Shannon diversity index
G
% CD27+ / DOT cells
% CD27+ / CD3+Vδ1+ cells
100
80
60
40
20
0
HD#1
HD#2
HD#3
HD#4

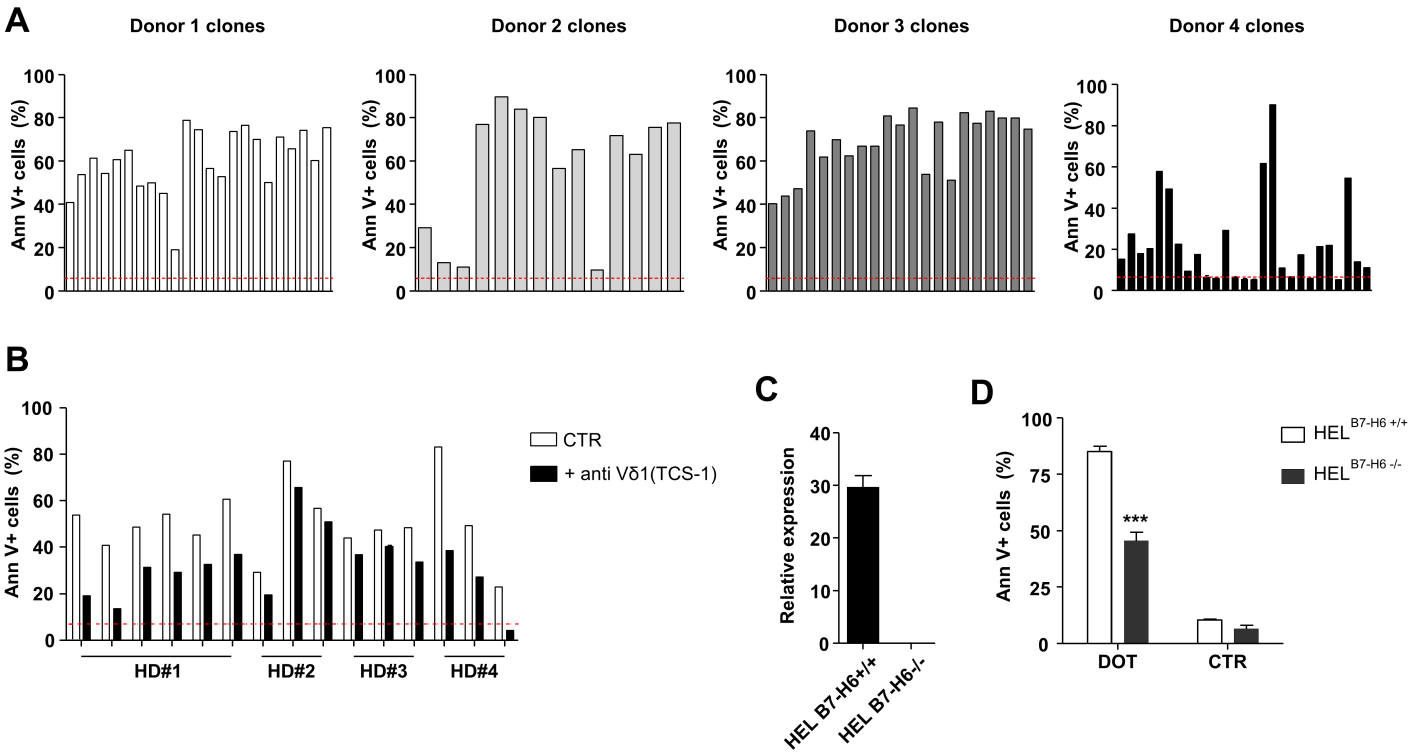
A
Donor 1 clones
Donor 2 clones
Donor 3 clones
Donor 4 clones
Ann V+ cells (%)
100
80
60
40
20
0
B
CTR
+ anti Vδ1(TCS-1)
HD#1
HD#2
HD#3
HD#4
C
Relative expression
40
30
20
10
0
HEL B7-H6+/+
HEL B7-H6-/-
D
HEL B7-H6 +/+
HEL B7-H6 -/-
75
50
25
***
DOT
CTR

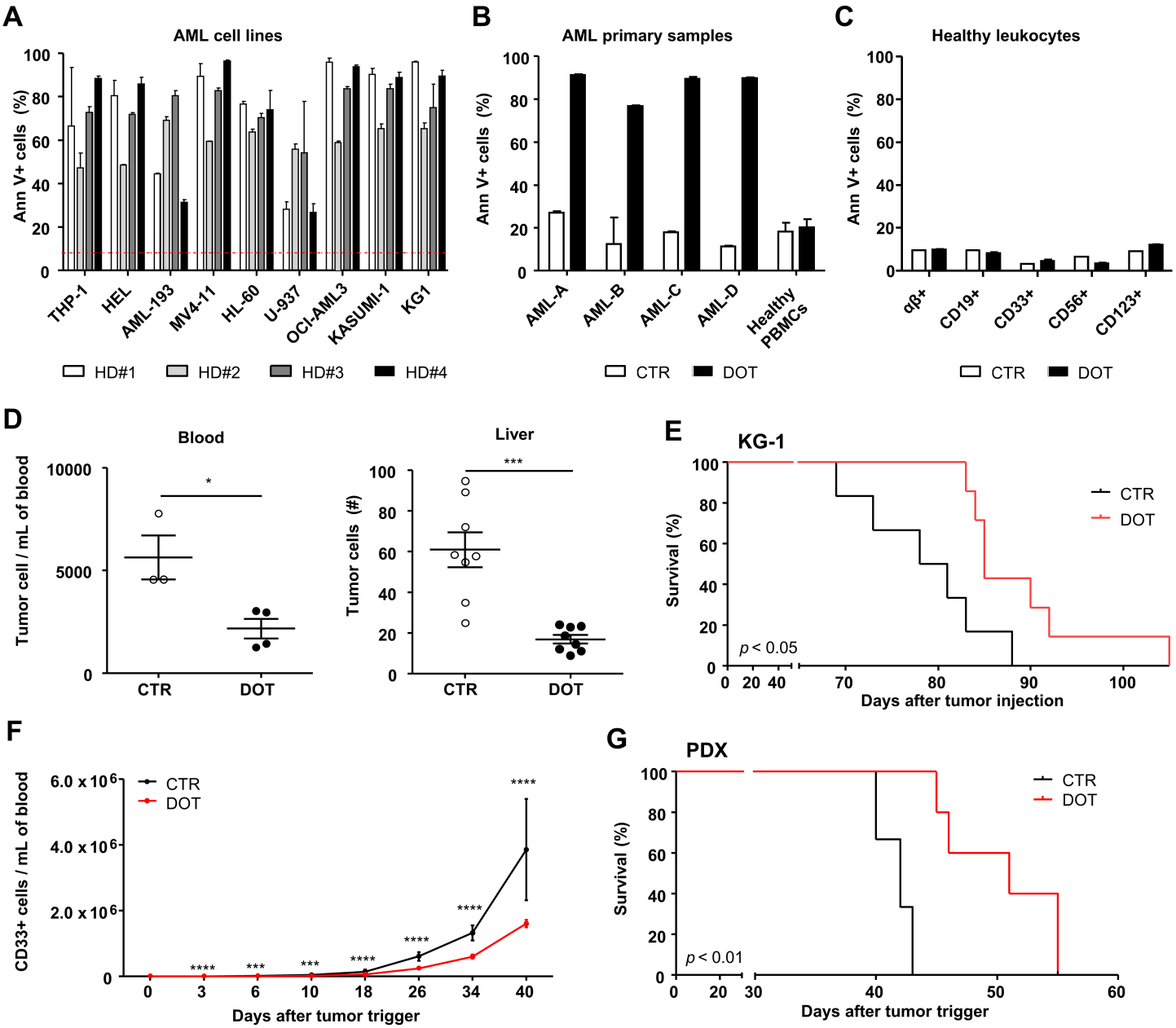
A
AML cell lines
Ann V+ cells (%)
THP-1
HEL
AML-193
MV4-11
HL-60
U-937
OCI-AML3
KASUMI-1
KG1
HD#1
HD#2
HD#3
HD#4
B
AML primary samples
AML-A
AML-B
AML-C
AML-D
Healthy PBMCs
CTR
DOT
C
Healthy leukocytes
αβ+
CD19+
CD33+
CD56+
CD123+
D
Blood
Tumor cell / mL of blood
Liver
Tumor cells (#)
E
KG-1
Survival (%)
p < 0.05
Days after tumor injection
F
CD33+ cells / mL of blood
Days after tumor trigger
G
PDX
p < 0.01

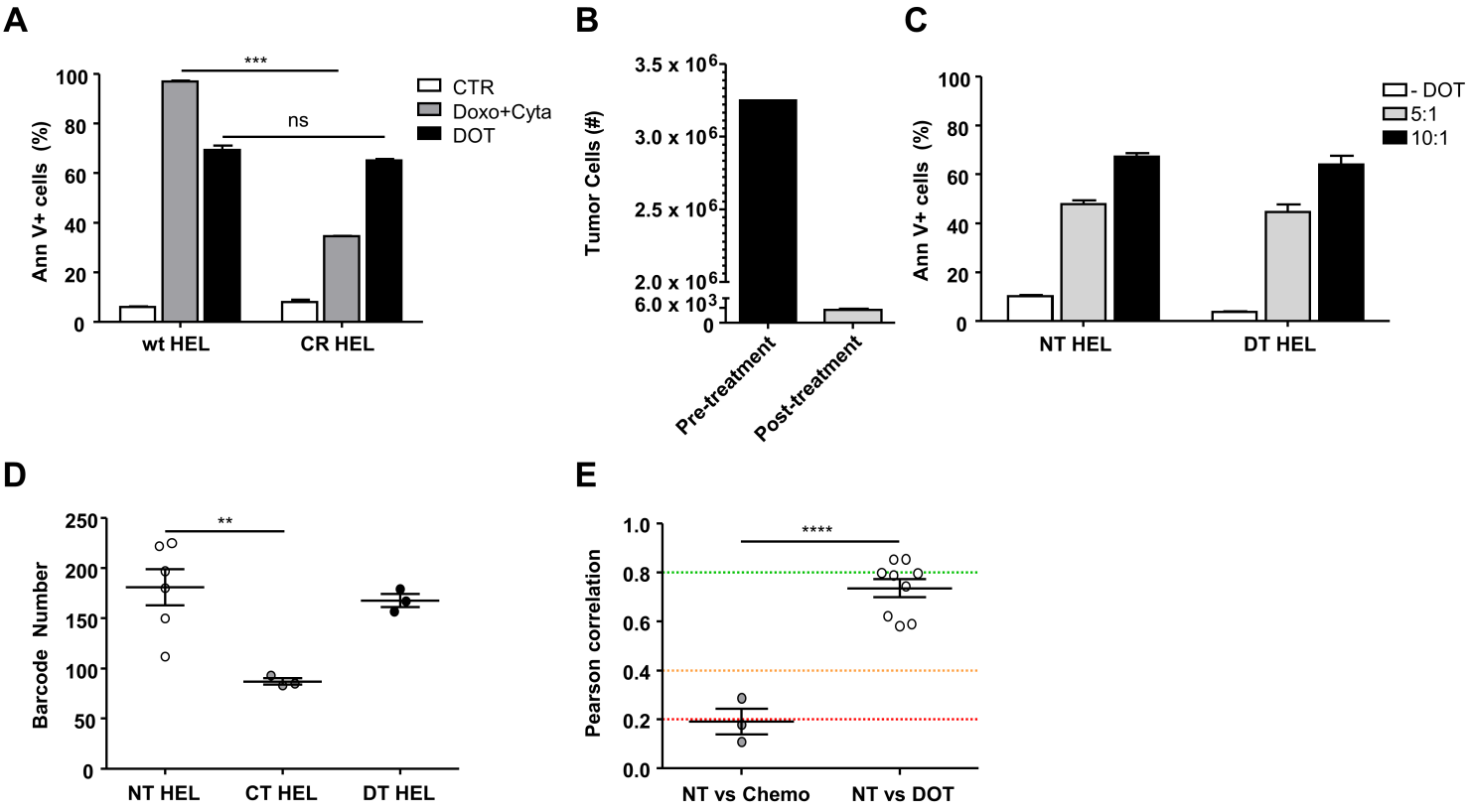
A
***
ns
CTR
Doxo+Cyta
DOT
Ann V+ cells (%)
100
80
60
40
20
0
wt HEL
CR HEL
B
Tumor Cells (#)
3.5 x 10^6
3.0 x 10^6
2.5 x 10^6
2.0 x 10^6
6.0 x 10^3
0
Pre-treatment
Post-treatment
C
- DOT
5:1
10:1
Ann V+ cells (%)
NT HEL
DT HEL
D
**
Barcode Number
250
200
150
100
50
0
NT HEL
CT HEL
DT HEL
E
****
Pearson correlation
1.0
0.8
0.6
0.4
0.2
0.0
NT vs Chemo
NT vs DOT